Exchange Interactions in Di-μ-hydroxo-bis[bis(1,2-diaminoethane)-chromium(III)] Salts. Structural, Magnetochemical, and Optical Spectroscopic Investigations

By **Adrian Beutler, Hans U. Güdel,*** and **Timothy R. Snellgrove,** Department of Chemistry, University of Bern, Switzerland
Gervais Chapuis and **Kurt J. Schenk,** Department of Crystallography, University of Lausanne, Switzerland

Chloride, bromide, iodide, and dichloride diperchlorate salts of the title complex have been prepared. The crystal structures of $[Cr_2(OH)_2(en)_4]Cl_4 \cdot 2H_2O$ and $[Cr_2(OH)_2(en)_4]Br_4 \cdot 2H_2O$ have been determined by single-crystal *X*-ray measurements on an automatic diffractometer, and refined to *R* 0.023 for the chloride and 0.031 for the bromide. Lattice constants are a = 8.165 0(8), b = 8.740 0(9), c = 9.790 2(7) Å, α = 67.196(7), β = 87.937(7), and γ = 64.587(7)° for the chloride, and a = 8.211(2), b = 8.980(1), c = 10.024(1) Å, α = 67.57(1), β = 88.90(1), and γ = 65.07(2)° for the bromide. Both structures belong to space group $P\bar{1}$ and are strictly isomorphous. The symmetry of the dichromium complex is $2/m$ in both salts. Moreover, a normal probability plot analysis shows the cations to be identical in the two compounds. Powder magnetic-susceptibility data have been collected for all the four complexes between 1.5 K and room temperature. Single-crystal and Nujol-mull absorption spectra have been recorded between 7 and 40 K in the region of transitions from the electronic ground state $^4A_2{}^4A_2$ to the lowest levels of the first singly excited state $^4A_2{}^2E$, and powder luminescence spectra obtained at <10 K. From the absorption and luminescence spectra the exchange splitting of the electronic ground state can be accurately determined. The exchange parameters J thus derived deviate by up to 10% from those obtained by fitting the magnetic-susceptibility data. These discrepancies indicate a slight temperature dependence of J. The values obtained for the biquadratic exchange parameter j from the magnetochemical fit have little if any physical significance. The exchange parameters (cm^{-1}) for the four salts, determined spectroscopically at <40 K, are: $J = 31.4 \pm 0.4$ and $j = 0.08 \pm 0.02$ (chloride), 30.0 ± 0.3 and $j = 0.11 \pm 0.08$ (bromide), 24.3 ± 0.9 and $j = 0.08 \pm 0.2$ (iodide), and 22.2 ± 0.2 and $j = 1.12 \pm 0.6$ (dichloride diperchlorate dihydrate).

A BIG effort is currently being made to obtain a better understanding of the electronic ground-state properties of binuclear chromium(III) complexes. A large number of di-μ-hydroxo-complexes of the general formula $[Cr_2(OH)_2L_4]$ have been synthesized and characterized by *X*-ray diffraction and magnetochemical techniques.[1] The aim of these investigations is to reveal correlations between structural and magnetic properties in a series of compounds, which could then be rationalized in terms of a theoretical model.[1,2] A remarkably simple dependence of the singlet–triplet separation on the Cu–O–Cu bridging angle has been found [3] in a series of copper complexes $[Cu_2(OH)_2L_4]$. In the di-μ-hydroxo-chromium complexes the situation is more complex: although the substances studied so far exhibit a strong dependence of the exchange splitting on the structural parameters, in particular the Cr–O–Cr angle, it has not yet been possible to derive a picture which would allow a theoretical analysis.[1] In the comparisons of complexes with different ligands L in $[Cr_2(OH)_2L_4]$ the basic assumption made was that changes in the chemical bonding, and thus the exchange splitting of the ground state associated with changing the ligands, are reflected by the structure of the $Cr(\mu\text{-}O)_2Cr$ group. However, vastly different values, ranging from 2 to 24 cm^{-1} $[\hat{H}_{ex} = J(\hat{S}_a \cdot \hat{S}_b)]$, of the isotropic bilinear exchange parameter J have been reported for $[Cr_2(OH)_2(en)_4]^{4+}$ (en = 1,2-diaminoethane) in different environments.[4,5] This is a surprising result, since we are used to considering the exchange interaction in binuclear complexes as an intramolecular property which is not greatly affected by crystal packing in a solid. Thus, in order to eliminate the main uncertainties inherent in the above assumption, it would be necessary to study the same complex in different crystal surroundings. As a contribution towards this goal we undertook a systematic investigation of the chloride, bromide, iodide, and mixed chloride perchlorate salts of the above cation using *X*-ray diffraction and magnetochemical as well as optical spectroscopic techniques. Of the series $[Cr_2(OH)_2(en)_4]X_n \cdot mH_2O$, the crystal structures for X = Cl or Br, $n = 4$, and $m = 2$ have been determined.

Measurement of the magnetic susceptibility over a wide temperature range is the most widely used method for determining ground-state splittings caused by exchange interactions in polynuclear transition-metal complexes. This bulk technique is very useful for the observation of trends in a series of complexes. The values of the exchange parameters obtained from fitting an empirical model to the susceptibility data must, however, be interpreted with some care, since there are a number of traps inherent in any procedure of extracting molecular parameters from bulk data. It is therefore desirable to use spectroscopic techniques to supplement the magnetochemical studies. Unfortunately, the number of chemical systems susceptible to spectroscopic study is rather limited. E.s.r. spectroscopy has found only limited application since the pioneering work of Bleaney and Bowers on copper(II) acetate.[6] Optical spectroscopy has been used for a number of polynuclear chromium(III) complexes to determine the ground-state splittings.[7,8] On the other hand, in the study of pairs of paramagnetic transition-metal ions created by doping diamagnetic host lattices both optical and e.s.r. spectroscopic methods are predominant.[9,10] Neutron inelastic scattering has recently been introduced in this field; by using this technique it was possible to observe transitions within the ground-state multiplet.[11,12] These measurements provided some evidence for a temperature dependence of the exchange splitting.

The present study has four main objectives: (*i*) to determine exchange splittings of the electronic ground state as accurately as possible by using spectroscopic techniques; (*ii*) to compare magnetochemical and spectroscopic exchange parameters and critically evaluate the magnetochemical procedure; (*iii*) to provide some new information on the temperature dependence of exchange; and (*iv*) to correlate electronic ground-state properties (exchange parameters) with structural parameters.

RESULTS AND DISCUSSION

Crystal Structures of Di-μ-hydroxo-bis[bis(1,2-diaminoethane)chromium(III)] *Chloride and Bromide Dihydrates.*—*The chloride.* From the shiny red-violet crystals a nearly isometric one was chosen. It was bounded by three pinacoids, {100}, {010}, and {001}, and the two bevel faces (011) and (101). Opposite faces were separated by 0.029, 0.022, and 0.020 cm respectively. An absorption correction was applied which yielded transmission factors between 0.712 and 0.802. Lattice constants of the triclinic crystal were obtained from a least-squares optimization of 25 accurately centred reflections, the diffractions angles, 2θ, of which lay between 45 and 50°. The calculated density, based on the assumption of one formula unit per unit cell, is in reasonably good agreement with the measured one, the latter being determined by flotation in benzene and methyl iodide at 23 °C. The space group is $P\bar{1}$, as indicated by the distribution of the normalized structure factors and confirmed by successful refinement.

At 23 °C, 3 404 reflections were collected up to $(\sin\theta)/\lambda = 0.732$, 339 of which had $I < 3\sigma(I)$ derived from counting statistics and the fluctuations of periodically measured check reflections. Three of the check reflections were found to be stable during the experiment. Weights assigned were $w(F) = 1/\sigma^2(F)$. The Patterson function yielded the positions of the chromium and the chlorine atoms. A subsequent F_0 map showed the remaining atoms of the dimer. The water molecule and the hydrogens were finally revealed by ΔF maps after successive cycles of full-matrix refinement. During the final anisotropic full-matrix refinement, where the number of reflections per parameter being optimized was 17.4, all atoms converged towards reasonable positions except for the hydroxo-hydrogen H(O1) and the two water hydrogens, H(1O2) and H(2O2). These three atoms were therefore fixed at the positions found on the difference map, only their U values being refined. After the last cycle no shift was larger than 1.21 times the error associated with the optimized co-ordinate; the average shift-to-error quotient was 0.22. The final residuals, based on $|F|$ values, were $R = (\Sigma|\Delta F|/\Sigma|F_0|) = 0.023$, $R' = (\Sigma|w\Delta F|/\Sigma|wF_0|) = 0.031$, and goodness of fit = $(\Sigma w\Delta F^2/\text{number of reflections} - \text{number of variables})^{\frac{1}{2}} = 2.665$. The final parameters are listed in Table 2. Structure-factor tables and thermal parameters for both salts are available as Supplementary Publication No. SUP 22460 (41 pp.).*

The bromide. The shiny red-violet crystal measured was bordered by four pinacoids, {100}, {010}, {001}, and {110}, and the pedion (011). Opposite faces were separated by 0.025, 0.011, 0.012, and 0.024 cm respectively. An absorption correction yielded transmission factors between 0.377 and 0.518. Lattice constants were determined from 25 reflections. The measured density, which was found by flotation in benzene and methyl iodide, agrees perfectly with one formula unit per unit cell. At 23 °C, 3 606 intensities were collected up to $(\sin\theta)/\lambda = 0.707$, 1 141 of which had $I < 3\sigma(I)$. No significant oscillation of three periodically measured check reflections could be detected. Inspection of the Patterson map revealed the chromium and anion positions to be almost the same as in the chloride salt, thus suggesting that the two complexes are strictly isomorphous. Indeed, the structure was refined successfully using the initial atomic positions of the chloride. The hydroxo-hydrogen H(O1) and the two water hydrogens, H(1O2) and H(2O2), could not be found on difference maps. They were therefore calculated according to the model of the chloride structure and held fixed at these positions, only their U values being refined. After anisotropic full-matrix refinement, no shift was larger than 0.31 times the error associated with the optimized parameter; the average shift-to-error quotient was 0.09. The final residuals, based on $|F|$ values, were $R = 0.031$, $R' = 0.029$, and goodness of fit = 2.106 6. The final parameters are in Table 5.

Discussion. Both structures are strictly isomorphous, as shown by the refinement of the bromide salt. They consist of $[Cr_2(OH)_2(en)_4]^{4+}$ dimers which are interrelated by abundant hydrogen bonding. The dimer is shown in Figure 1. For the chloride, the co-ordination of chromium is much distorted from octahedral, *cis* angles lying between 77.6 and 95.9°, *trans* between 166.3 and 171.9.° (For other angles see Tables 4 and 7.) The chromium complex is centrosymmetric. Moreover,

TABLE 1

Crystal data

	$[Cr_2(OH)_2(en)_4]Cl_4\cdot 2H_2O$	$[Cr_2(OH)_2(en)_4]Br_4\cdot 2H_2O$
a/Å	8.165 0(8)	8.211(2)
b/Å	8.740 0(9)	8.980(1)
c/Å	9.790 2(7)	10.024(1)
α/°	67.196(7)	67.57(1)
β/°	87.937(7)	88.90(1)
γ/°	64.587(7)	65.07(2)
U/Å³	574.55(9)	610.6(2)
Z	1	1
$F(000)$	290	362
Space group	$P\bar{1}$	$P\bar{1}$
D_m/g cm⁻³	1.587(5)	1.99(5)
D_c/g cm⁻³	1.607 6(3)	1.996 1(7)
λ(Mo-K_α)/Å	0.710 69	0.710 7
μ(Mo-K_α)/cm⁻¹	14.8	78.9

---

[*] For details see Notices to Authors No. 7, *J.C.S. Dalton*, 1978, Index issue.

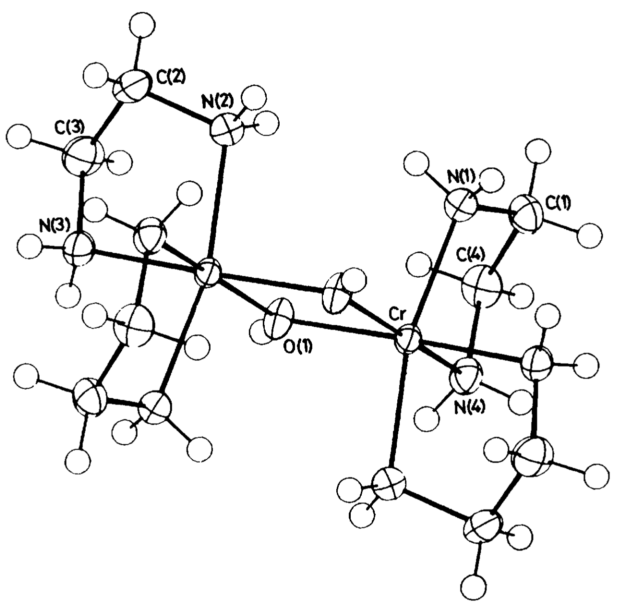

FIGURE 1 Structure of the $[Cr_2(OH)_2(en)_4]^{4+}$ cation occurring in the chloride and bromide salts. Atoms are represented by thermal ellipsoids enclosing 50% probability. Hydrogen atoms are on an arbitrary scale

it reveals, within experimental precision, a mirror plane perpendicular to the Cr–Cr line and containing the inversion centre. Thus the symmetry of the cation is 2/*m*. Other local symmetries of the $[Cr_2(OH)_2(en)_4]^{4+}$ complex have also been found.[5,13] Atoms N(4), Cr, O(1), and N(3) and those generated by the centre of symmetry at (0,0,0) very nearly constitute a plane; the standard deviation of the distances of the atoms from the calculated best plane is 0.051 Å. The water molecule also lies approximately in this plane, its hydrogen atoms being equivalent with reference to the mirror plane of the complex. The refined hydrogen positions yield reasonable O–H, N–H, and C–H distances, means: 0.76, 0.88, and 0.96 Å, a reasonable order, considering the electronegativities of O, N, and C.

TABLE 2

Atomic parameters of $[Cr_2(OH)_2(en)_4]Cl_4 \cdot 2H_2O$ with estimated standard deviations in parentheses

Atom	*X*	*Y*	*Z*
Cr	−0.041 75(3)	−0.053 92(2)	0.159 09(2)
O(1)	0.058 0(1)	−0.160 3(1)	0.015 4(1)
N(1)	0.211 5(2)	−0.116 3(2)	0.262 3(1)
N(2)	0.309 6(2)	0.003 9(2)	−0.107 7(1)
N(3)	0.168 5(2)	−0.095 8(2)	−0.286 8(1)
N(4)	0.011 9(2)	−0.312 2(2)	0.331 7(1)
C(1)	0.263 1(2)	−0.275 3(2)	0.410 8(2)
C(2)	0.421 2(2)	−0.054 1(2)	−0.218 1(2)
C(3)	0.371 0(2)	−0.189 1(2)	−0.242 9(2)
C(4)	0.210 7(2)	−0.412 6(2)	0.394 0(2)
Cl(1)	−0.383 10(5)	−0.359 79(5)	0.185 94(4)
Cl(2)	−0.141 99(5)	−0.217 01(5)	−0.374 58(4)
O(2)	0.184 2(3)	−0.506 6(2)	0.054 4(2)
H(O1)	0.083 3	−0.257 4	0.025 9
H(1N1)	0.206(2)	−0.022(2)	0.273(2)
H(2N1)	0.306(2)	−0.154(2)	0.215(2)
H(1N2)	0.317(2)	0.103(2)	−0.104(2)
H(2N2)	0.356(2)	−0.080(2)	−0.021(2)
H(1N3)	0.126(2)	0.172(2)	−0.277(2)
H(2N3)	0.141(2)	−0.016(3)	−0.388(2)
H(1N4)	−0.046(2)	−0.299(2)	0.403(2)
H(2N4)	−0.025(2)	−0.376(2)	0.295(2)
H(1C1)	0.199(2)	−0.234(2)	0.483(2)
H(2C1)	0.393(2)	−0.325(2)	0.444(2)
H(1C2)	0.549(3)	−0.108(2)	−0.183(2)
H(2C2)	0.390(2)	0.059(2)	−0.311(2)
H(1C3)	0.407(2)	−0.299(3)	−0.152(2)
H(2C3)	0.429(2)	−0.224(2)	−0.320(2)
H(1C4)	0.239(2)	−0.516(2)	0.485(2)
H(2C4)	0.278(2)	−0.462(2)	0.324(2)
H(1O2)	0.208 3	−0.532 6	−0.005 8
H(2O2)	0.166 7	−0.585 0	0.125 3

TABLE 3

Atomic distances (in Å) in the chloride

Cr–O(1$^{\mathrm{I}}$) [a]	1.940(1)	O(2)–H(O1)	1.87 [b]
Cr–O(1)	1.947(1)		
Cr–N(1)	2.086(1)	Cl(1)–H(1O2)	2.45 [b]
Cr–N(4)	2.096(1)	Cl(1)–H(2N1)	2.49(2)
Cr$^{\mathrm{I}}$–N(2)	2.078(1)	Cl(1)–H(1N2)	2.36(2)
Cr$^{\mathrm{I}}$–N(3)	2.088(2)	Cl(1)–H(2N2)	2.57(1)
Cr$^{\mathrm{I}}$–Cr	3.029 8(4)		
O(1)–O(1$^{\mathrm{I}}$)	2.435(1)	Cl(2)–H(2O2)	2.45 [b]
N(1)–C(1)	1.482(2)	Cl(2)–H(1N1)	2.50(2)
C(1)–C(4)	1.499(3)	Cl(2)–H(1N3)	2.65(2)
C(4)–N(4)	1.487(2)	Cl(2)–H(2N3)	2.43(2)
N(2)–C(2)	1.488(2)	Cl(2)–H(1N4)	2.55(2)
C(2)–C(3)	1.503(3)		
C(3)–N(3)	1.485(2)		
O(1)–H(O1)	0.746 [b]		
O(2)–H(1O2)	0.704 [b]		
O(2)–H(2O2)	0.825 [b]		

[a] Roman numeral superscript indicates position generated by centre of inversion at (0,0,0). [b] Not refined, therefore no standard deviation.

TABLE 4

Bond angles (°) in the chloride

O(1)–Cr–N(1)	95.50(5)	Cr–N(1)–C(1)	109.6(1)
N(1)–Cr–N(4)	81.59(5)	N(1)–C(1)–C(4)	107.7(1)
N(1)–Cr–N(3$^{\mathrm{I}}$) [a]	88.46(5)	C(1)–C(4)–N(4)	107.3(1)
N(1)–Cr–O(1$^{\mathrm{I}}$)	95.20(5)	C(4)–N(4)–Cr	108.4(1)
O(1)–Cr–O(1$^{\mathrm{I}}$)	77.58(4)		
O(1)–Cr–N(4)	93.31(5)	Cr$^{\mathrm{I}}$–N(2)–C(2)	109.6(1)
N(4)–Cr–N(3$^{\mathrm{I}}$)	94.28(5)	N(2)–C(2)–C(3)	107.3(1)
O(1$^{\mathrm{I}}$)–Cr–N(3$^{\mathrm{I}}$)	95.04(5)	C(2)–C(3)–N(3)	107.0(1)
O(1)–Cr–N(2$^{\mathrm{I}}$)	95.90(5)	C(3)–N(3)–Cr$^{\mathrm{I}}$	110.1(1)
O(1$^{\mathrm{I}}$)–Cr–N(2$^{\mathrm{I}}$)	94.73(5)		
N(3$^{\mathrm{I}}$)–Cr–N(2$^{\mathrm{I}}$)	81.22(6)	O(1)–H(O1)–O(2)	171.2 [b]
N(4)–Cr–N(2$^{\mathrm{I}}$)	90.11(5)		
		O(2)–H(1O2)–Cl(1)	163 [b]
O(1)–Cr–N(3$^{\mathrm{I}}$)	171.87(3)	N(1)–H(2N1)–Cl(1)	157(1)
O(1$^{\mathrm{I}}$)–Cr–N(4)	170.06(4)	N(2)–H(1N2)–Cl(1)	156(2)
N(1)–Cr–N(2$^{\mathrm{I}}$)	166.26(5)	N(2)–H(2N2)–Cl(1)	156(2)
Cr–O(1)–Cr$^{\mathrm{I}}$	102.424(47)	O(2)–H(2O2)–Cl(2)	164 [b]
		N(1)–H(1N1)–Cl(2)	162(2)
H(1O2)–O(2)–H(2O2)	112.5 [b]	N(3)–H(1N3)–Cl(2)	145(1)
		N(3)–H(2N3)–Cl(2)	161(2)
		N(4)–H(1N4)–Cl(2)	160(2)

[a] Roman numeral superscript indicates position generated by centre of inversion at (0,0,0). [b] Not refined, therefore no standard deviation.

The hydrogen-bonding scheme is shown in Figure 2. A distance criterion[14] states that in an arrangement of the type X–H · · · Y a hydrogen bond H · · · Y may exist if the distance of H from Y is considerably shorter than the sum of the van der Waals radii of H and of Y. These radii are[15] 1.2, 1.5, 1.4, 1.8, and 1.95 Å for H, N, O, Cl, and Br respectively. Thus an H · · · O hydrogen bond should be <2.6 Å, an H · · · Cl bond <3 Å, and an H · · · Br bond <3.15 Å. With this knowledge the nine hydrogen–chlorine distances lying in the range

2.36—2.65 Å may well be claimed to be hydrogen bonds. (For distances see Tables 3 and 6.) Finally, the short distance of 1.87 Å between H(O1) and O(2) indicates a H • • • O bond. All oxygen–hydrogen and all but one nitrogen–hydrogen [H(2N4): nearest electron donor 3.07 Å away] bonds participate in the hydrogen-bonding scheme.

TABLE 5

Atomic parameters of $[Cr_2(OH)_2(en)_4]Br_4{\cdot}2H_2O$

Atom	*X*	*Y*	*Z*
Cr	−0.041 96(7)	−0.050 53(6)	0.154 86(5)
O(1)	0.053 5(3)	−0.155 1(3)	0.015 5(2)
N(1)	0.210 8(4)	−0.116 9(4)	0.259 9(3)
N(2)	0.307 8(4)	−0.001 3(4)	−0.100 2(3)
N(3)	0.166 4(4)	−0.097 7(5)	−0.276 4(3)
N(4)	0.005 1(4)	−0.298 1(4)	0.322 5(3)
C(1)	0.257 5(5)	−0.267 5(5)	0.406 6(4)
C(2)	0.420 6(5)	−0.059 9(5)	−0.205 3(4)
C(3)	0.368 8(5)	−0.191 3(5)	−0.230 0(4)
C(4)	0.201 6(5)	−0.398 9(5)	0.388 1(4)
Br(1)	−0.370 44(5)	−0.371 94(5)	0.192 13(4)
Br(2)	−0.160 06(5)	−0.209 27(5)	−0.380 55(4)
O(2)	0.179 0(6)	−0.495 3(4)	0.059 8(4)
H(1N1)	0.207(4)	−0.041(4)	0.273(3)
H(2N1)	0.297(5)	−0.145(4)	0.203(3)
H(1N2)	0.312(4)	0.091(4)	−0.095(3)
H(2N2)	0.349(5)	−0.077(5)	−0.012(4)
H(1N3)	0.125(6)	−0.188(6)	−0.269(4)
H(2N3)	0.142(6)	−0.030(5)	−0.349(4)
H(1N4)	−0.070(5)	−0.260(5)	0.387(4)
H(2N4)	−0.035(5)	−0.336(5)	0.280(4)
H(1C1)	0.188(4)	−0.219(4)	0.479(3)
H(2C1)	0.389(6)	−0.307(5)	0.433(4)
H(1C2)	0.534(6)	−0.104(6)	−0.166(5)
H(2C2)	0.374(5)	0.079(5)	−0.300(4)
H(1C3)	0.411(5)	−0.319(5)	−0.134(4)
H(2C3)	0.435(5)	−0.239(4)	−0.303(4)
H(1C4)	0.225(6)	−0.504(6)	0.482(5)
H(2C4)	0.271(5)	−0.447(5)	0.313(4)

TABLE 6

Atomic distances (in Å) in the bromide

Cr–O(1$^{\mathrm{I}}$) *	1.946(2)	Br(1)–H(2N1)	2.67(3)
Cr–O(1)	1.946(2)	Br(1)–H(1N2)	2.58(4)
Cr–N(1)	2.082(4)	Br(1)–H(2N2)	2.72(3)
Cr–N(4)	2.089(3)		
Cr$^{\mathrm{I}}$–N(2)	2.068(4)	Br(2)–H(1N1)	2.72(4)
Cr$^{\mathrm{I}}$–N(3)	2.084(4)	Br(2)–H(1N3)	2.72(5)
Cr$^{\mathrm{I}}$–Cr	3.038 4(8)	Br(2)–H(2N3)	2.79(4)
O(1)–O(1$^{\mathrm{I}}$)	2.432(3)	Br(2)–H(1N4)	2.57(4)
N(1)–C(1)	1.485(4)		
C(1)–C(4)	1.504(7)		
C(4)–N(4)	1.487(5)		
N(2)–C(2)	1.490(5)		
C(2)–C(3)	1.511(8)		
C(3)–N(3)	1.496(5)		

* Roman numeral superscript indicates position generated by centre of inversion at (0,0,0).

TABLE 7

Bond angles (°) in the bromide

O(1)–Cr–N(1)	95.7(1)	Cr–N(1)–C(1)	110.0(3)
N(1)–Cr–N(4)	81.4(1)	N(1)–C(1)–C(4)	106.6(3)
N(1)–Cr–N(3$^{\mathrm{I}}$) *	89.0(1)	C(1)–C(4)–N(4)	107.3(3)
N(1)–Cr–O(1$^{\mathrm{I}}$)	95.6(1)	C(4)–N(4)–Cr	108.8(3)
O(1)–Cr–O(1$^{\mathrm{I}}$)	77.4(1)		
O(1)–Cr–N(4)	93.5(1)	Cr$^{\mathrm{I}}$–N(2)–C(2)	110.2(3)
N(4)–Cr–N(3$^{\mathrm{I}}$)	94.4(1)	N(2)–C(2)–C(3)	106.8(4)
O(1$^{\mathrm{I}}$)–Cr–N(3$^{\mathrm{I}}$)	94.6(1)	C(2)–C(3)–N(3)	106.7(3)
O(1)–Cr–N(2$^{\mathrm{I}}$)	95.2(1)	C(3)–N(3)–Cr$^{\mathrm{I}}$	110.3(3)
O(1$^{\mathrm{I}}$)–Cr–N(2$^{\mathrm{I}}$)	94.7(1)		
N(3$^{\mathrm{I}}$)–Cr–N(2$^{\mathrm{I}}$)	81.3(2)	N(1)–H(2N1)–Br(1)	147(2)
N(4)–Cr–N(2$^{\mathrm{I}}$)	89.9(1)	N(2)–H(1N2)–Br(1)	154(3)
		N(2)–H(2N2)–Br(1)	149(3)
O(1)–Cr–N(3$^{\mathrm{I}}$)	171.33(9)	N(1)–H(1N1)–Br(2)	166(3)
O(1$^{\mathrm{I}}$)–Cr–N(4)	170.1(1)	N(3)–H(1N3)–Br(2)	140(2)
N(1)–Cr–N(2$^{\mathrm{I}}$)	166.4(1)	N(3)–H(2N3)–Br(2)	162(5)
Cr–O(1)–Cr$^{\mathrm{I}}$	102.64(11)	N(4)–H(1N4)–Br(2)	159(3)

* Roman numeral superscript denotes position generated by centre of inversion at (0,0,0).

The bromide parameters are very similar to those of the chloride. The cation has, within experimental precision, 2/*m* symmetry. The standard deviation of the N(3),Cr,O,N(4) plane is 0.054. Average values of the N–H and C–H bonds are 0.85 and 1.02 Å respectively. The nine hydrogen–bromine distances (2.57—2.79 Å) are short enough to be hydrogen bonds. Hydrogen bonding between O(1) and O(2) and Br must be judged by another, less precise criterion,[14] since none of the hydrogens on oxygen has been located. Thus a hydrogen bond is assumed to be present if the distances between X and Y in the arrangement X–H • • • Y is slightly shorter than

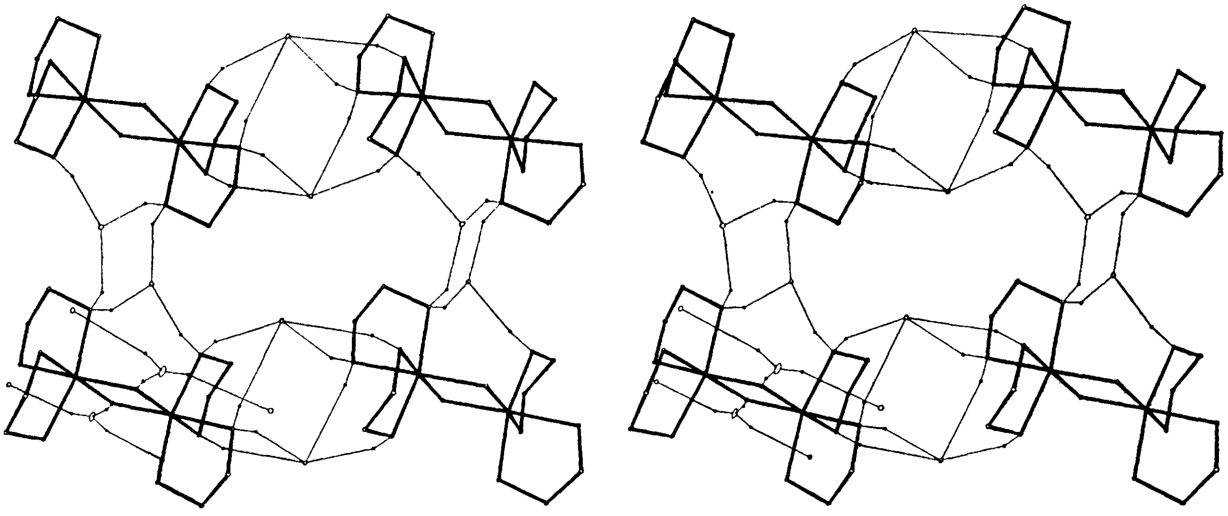

FIGURE 2 Stereoscopic representation of the N–H • • • Cl hydrogen-bonding scheme as viewed along *ac*. In the lower left corner, there are also shown the O–H • • • Cl bonds relating the *ac* layers

the sum of the van der Waals radii of X and Y. With a O(1)–O(2) distance of 2.63 Å, an average O(2)–Br distance of 3.32 Å, and H(2N4) 3.41 Å away from its nearest electron donor, it is obvious that similar hydrogen bonding exists, in the chloride and bromide salts.

Considering the delicate dependence of exchange interactions on Cr–O–Cr bridging angles, the reliability of the standard deviations of the corresponding parameters is crucial. In order to investigate the reliability of these standard deviations, which were derived from the least-squares procedure and the dispersions of the lattice constants, 47 pairs of distances and 70 pairs of angles in the cations of the two derivatives were subjected to a normal probability plot analysis.[16,17] Thus the moduli of the weighted deviations [equation (1)] were calculated

$$\delta m_i = \frac{\mathrm{P}(1)_i - \mathrm{P}(2)_i}{\{s^2[P(1)_i] + s^2[P(2)_i]\}^{\frac{1}{2}}} \qquad (1)$$

(1 refers to the chloride, 2 to the bromide, $i = 1$—117, and s = standard deviation of the parameter P). The 117 $|\delta m|$ values were arranged in order of increasing magnitude and the empirical cumulative distribution

$$\frac{2(2n - i) + 1}{2(2n)};\ n = 117 \qquad (2)$$

function (2) was determined. The quantile belonging to this value of the normal distribution function gives to a fair approximation the expected value of the ith element of the order statistic. The $|\delta m|$ values were plotted against their expected values (Figure 3). The overall feature of this graph is fairly linear, only its tail being slightly bent. Knowing that little significance should be attached to the tail,[16,17] we may disregard the 16 values of $|\delta m|$ which are larger than 3.5 (range 3.57—9.62). The graph is distinctly linear up to $|\delta m| = 2.5$, while the remaining points suggest the bending of the tail. The correlation coefficient of the total graph is 0.997, its gradient 2.18(2), and its ordinate intersection —0.08(10). The standard deviations were thus underestimated by a factor of 2.18 on the average. After correction by this factor, the largest deviation $|\delta m|$ becomes a more reasonable 4.41. From the linearity of the function we may conclude that the $|\delta m|$ values are normally distributed and that therefore the differences between corresponding parameters in the two cations are essentially due to random errors and can therefore be considered as non-significant.

Magnetochemical and Spectroscopic Investigations.—The determination of exchange parameters by absorption and luminescence spectroscopy can yield accurate results if transitions from and to individual levels of the ground state can be resolved.[7-9] In the present study the magnetic-susceptibility data were first used to obtain the order of magnitude of the exchange splitting. Then the optical spectroscopic data were used to determine the ground-state splittings as accurately as possible. In order to arrive at a critical evaluation of the fitting procedure commonly used to determine exchange parameters from magnetic-susceptibility data,[5] we fitted our susceptibility data to several empirical Hamiltonians containing from one to three adjustable parameters. The results of these fits were then compared with the spectroscopically determined splittings. Since the spectroscopic splittings were all determined at <40 K this comparison provides some information about the temperature dependence of the exchange.

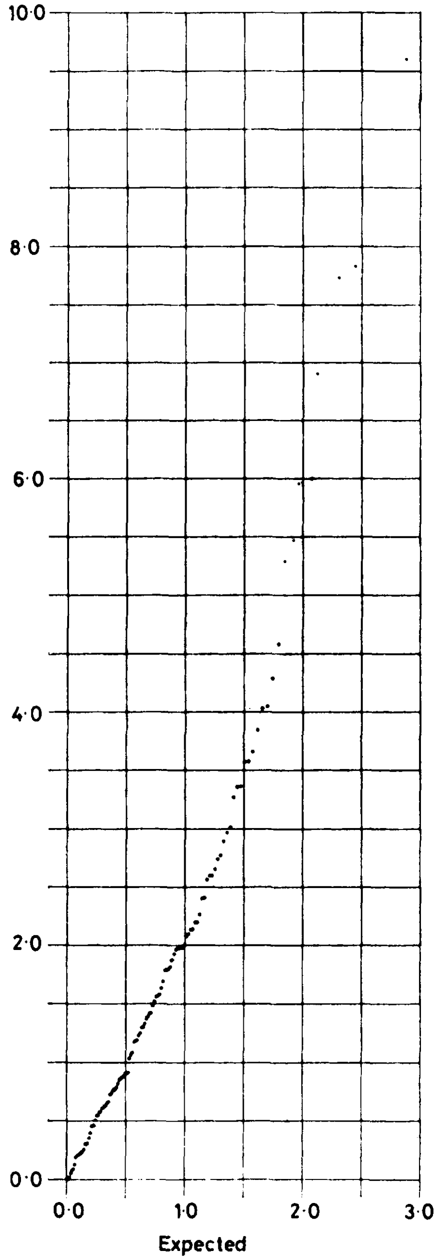

FIGURE 3 Half-normal probability plot comparing 117 pairs of parameters of the dichromium complexes in the chloride and bromide salts. The moduli of the weighted deviations are plotted against the expected values

Spectroscopic transitions were observed between the split manifold of the electronic ground state ${}^4A_2{}^4A_2$ and the lowest levels of the first singly excited state ${}^4A_2{}^2E$. The splitting of the first excited state will be the subject of a further investigation. Theory predicts the $^4A_2{}^2E$ state to be split by exchange interactions into eight levels, four having $S = 1$ and four $S = 2$.[9] At this

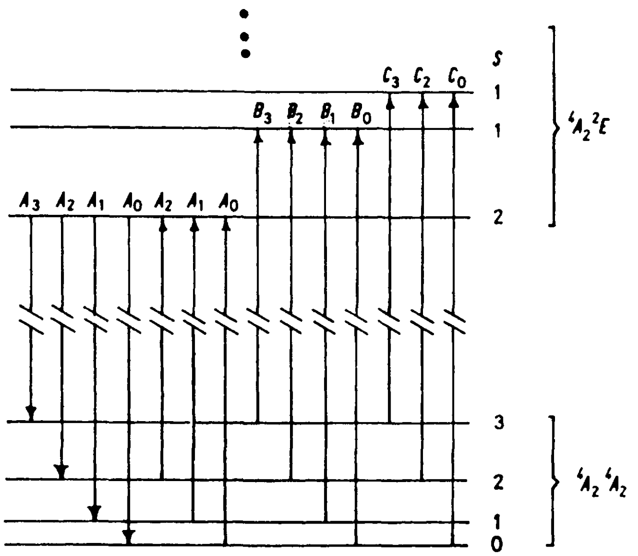

FIGURE 4 Schematic representation of the exchange splitting in the electronic ground state $^4A_2{}^4A_2$ and the lower part of the $^4A_2{}^2E$ manifold. All the transitions indicated by arrows ($\uparrow$ = absorption, $\downarrow$ = luminescence) were used to determine the ground-state splitting

preliminary stage the three lowest levels of the $^4A_2{}^2E$ manifold appear to be as shown schematically in Figure 4. It is clear from Figure 4 that the ground-state splitting pattern can either be determined from a luminescence experiment or from the temperature dependence of the corresponding absorption transitions.

Table 8 contains the J parameters obtained from fitting the magnetic-susceptibility data with a Heisenberg-type Hamiltonian (3) containing the bilinear exchange constant J as the only adjustable parameter. Table 9 illustrates the effect of introducing additional adjustable

$$\hat{H}_{ex} = J(\hat{S}_a . \hat{S}_b) \qquad (3)$$

parameters into the fitting Hamiltonian. We conclude that the values obtained for the biquadratic exchange parameter j have little if any physical significance. The g values are reasonable. J can be determined with an accuracy of a few percent. The changes in J in going from a model with one parameter to models with more parameters are several times the calculated standard deviations. This tends to invalidate the use of the standard deviation as an indicator of the accuracy of the parameter. These conclusions will be underlined by a comparison with the spectroscopic results.

TABLE 8

Results of fitting the magnetic-susceptibility data with the Hamiltonian $\hat{H}_{ex} = J(\hat{S}_a . \hat{S}_b)$ ($g = 2.0$)

Complex	J/cm^{-1}
$[(en)_2Cr(OH)_2Cr(en)_2]Cl_4 \cdot 2H_2O$	31.0 ± 0.1
$[(en)_2Cr(OH)_2Cr(en)_2]Br_4 \cdot 2H_2O$	29.5 ± 0.2
$[(en)_2Cr(OH)_2Cr(en)_2]I_4$	23.8 ± 0.1
$[(en)_2Cr(OH)_2Cr(en)_2]Cl_2[ClO_4]_2 \cdot 2H_2O$	27.3 ± 0.1

Figures 5 and 6 show two typical examples of single-crystal and Nujol-mull absorption spectra in the region of the first transitions $^4A_2{}^4A_2 \rightarrow {}^4A_2{}^2E$. The corresponding powder-emission spectra, which are also typical for the whole series, are given in Figures 7 and 8. The three lowest transitions in the absorption spectra are seen to exhibit different temperature dependences of their

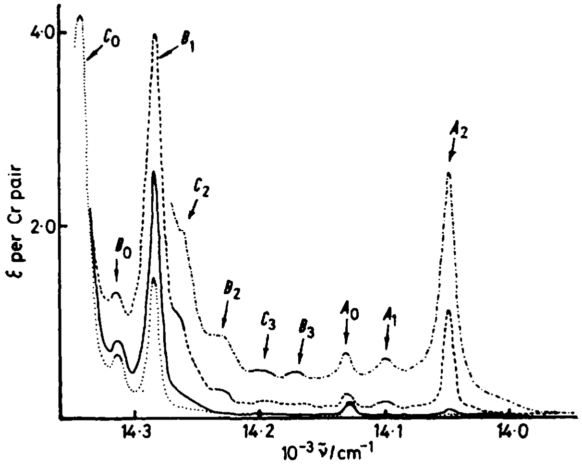

FIGURE 5 Low-temperature single-crystal absorption spectra of $[(en)_2Cr(OH)_2Cr(en)_2]Cl_2[ClO_4]_2 \cdot 2H_2O$ in the region of electronic transitions to the lowest levels of the first excited state $^4A_2{}^2E$. The spectra were recorded at 9.5 (· · · ·), 13.5 (——), 24.5 (— — —), and 42 K (— · — · —). All the spectra were measured perpendicular to the well developed large faces of the crystals. With this set up the linear dichroism of the absorption bands was found to be very small. Based on their positions and temperature dependences, the bands are assigned to the transitions in Figure 4

TABLE 9

Results of fitting the magnetic-susceptibility data of $[(en)_2Cr(OH)_2Cr(en)_2]I_4$ with models containing one to three adjustable parameters. In fits 1 and 3, g was set equal to 2.0. $R = \left[\sum_{i=1}^{n} (Y_{calc.} - Y_{expt.})_i^2 \Big/ \sum_{i=1}^{n} Y_{expt.i}^2\right]^{\frac{1}{2}}$ is a measure of the goodness of the least-squares fit. The number of experimental points is 88

Fit	Hamiltonian	Number of adjustable parameters	$\frac{J}{cm^{-1}}$	$\frac{j}{cm^{-1}}$	g	R
1	$\hat{H}_{ex} = J(\hat{S}_a \cdot \hat{S}_b)$	1	23.8 ± 0.10			0.017 3
2	$\hat{H}_{ex} = J(\hat{S}_a \cdot \hat{S}_b)$	2	22.6 ± 0.18		1.977 ± 0.003	0.013 9
3	$\hat{H}_{ex} = J(\hat{S}_a \cdot \hat{S}_b) - j(\hat{S}_a \cdot \hat{S}_b)^2$	2	24.1 ± 0.19	−0.22 ± 0.10		0.016 8
4	$\hat{H}_{ex} = J(\hat{S}_a \cdot \hat{S}_b) - j(\hat{S}_a \cdot \hat{S}_b)^2$	3	21.5 ± 0.37	0.36 ± 0.11	1.967 ± 0.004	0.013 1

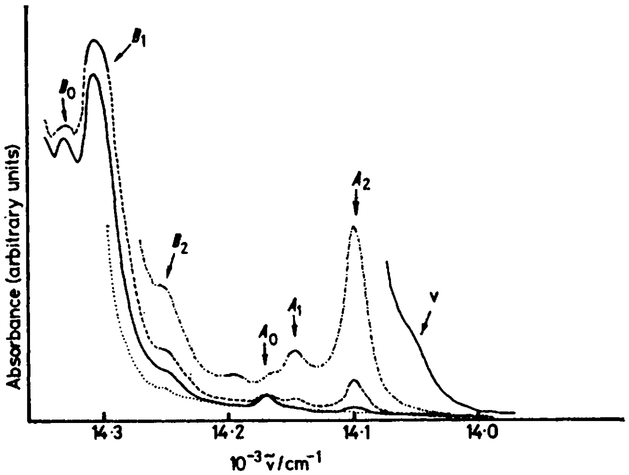

FIGURE 6 As for Figure 5, but for a Nujol mull of $[(en)_2Cr(OH)_2Cr(en)_2]I_4$. The spectra were recorded at 6.6 (· · · ·), 9.0 (——), 11.4 (— — —), 16.5 (— · — · —), and 29.5 K (——), rightmost curve. The shoulder denoted V is identified as a vibronic hot band

intensities. They must therefore originate in different ground-state levels. The luminescence spectra of all the four complexes are dominated by a very strong origin followed by a large number of well resolved side bands of much lower intensity. The origin is always coincident with a prominent absorption band (designated A2 in Figures 4—6), which, from its temperature dependence, belongs to a transition originating in $S = 2$. The assignment of this band as the electronic origin of the $S = 2 \longleftrightarrow S = 2$ transition A2 as shown in Figure 4 is therefore straightforward. Most of the other bands in the luminescence spectra of Figures 7 and 8 are vibronic side bands. The displacements from the origin of the majority of the side bands coincide with absorption bands in the i.r. spectrum. They must be assigned as vibronic origins. Our emphasis here is on the electronic

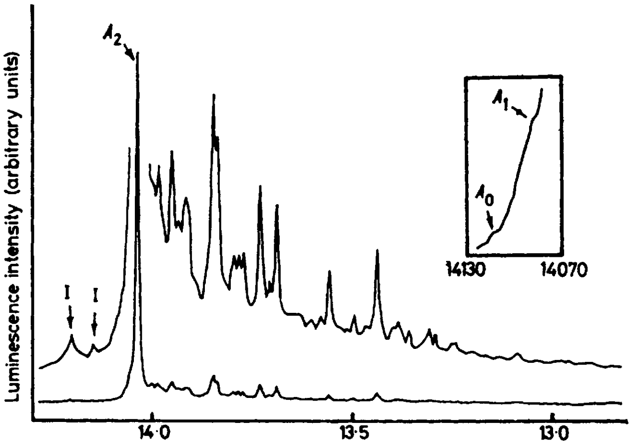

FIGURE 7 Luminescence spectrum at 9 K of a powder of $[(en)_2Cr(OH)_2Cr(en)_2]Cl_2[ClO_4]_2\cdot 2H_2O$. The prominent bands at 14 043 and 14 130 cm^{-1} containing the electronic origins of two spin-forbidden transitions are enlarged in the insert. Two very weak bands marked I are impurity bands

properties of the ground state. No detailed analysis of the side-band structure is therefore given.

When the high-energy tail of the strong electronic origin in the luminescence spectra is measured with high resolution and sensitivity two very weak shoulders (insert in Figure 7) occur coincident with two weak bands in the absorption spectra. Owing to their intensities and their temperature dependence in the absorption spectra, they have to be assigned to electronic origins of the singly and doubly spin-forbidden transitions A1 and A0. The spin-forbidden transition A3 is difficult to identify unambiguously. There are bands in the luminescence spectra at positions where A3 is expected on the bases of the A0, A1, and A2 positions, but there is no independent experimental criterion to distinguish them from vibronic side bands. The absorption spectra at >60 K, where the $S = 3$ ground-state level should become thermally populated, are too broad to make assignments. In some of the absorption spectra, transitions to the B and C levels of the first excited state are resolved. Table 10 contains all the spectroscopic data used in determining the ground-state splittings. In Table 11 the exchange parameters J and j, obtained from fitting the observed splittings of Table 10 to the exchange Hamiltonian (4), are compared with the

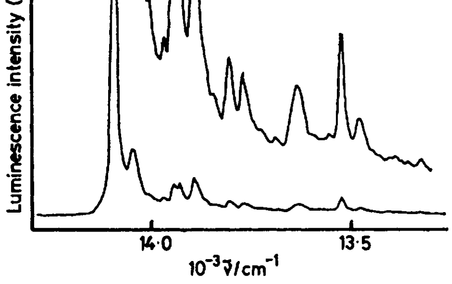

FIGURE 8 As for Figure 5, but for $[(en)_2Cr(OH)_2Cr(en)_2]I_4$

$$\hat{H}_{ex} = J(\hat{S}_a \,.\, \hat{S}_b) - j(\hat{S}_a \,.\, \hat{S}_b)^2 \qquad (4)$$

corresponding values obtained from the least-squares fit of the magnetic-susceptibility data. The differences between the two sets of J parameters are of the order of 10%. Given all the problems inherent in the magnetochemical procedure, this agreement is quite reasonable.

Except for the chloride perchlorate salt, which, as revealed by the magnetic-susceptibility data, appears to undergo a phase transition between 40 and 60 K, all the spectroscopically determined J values are larger than those obtained from the fit to the susceptibility. This is illustrated in Figure 9 by a comparison of the suscepti-

TABLE 10

Transitions observed between 7 and 40 K in absorption and luminescence, and the resulting ground-state splittings. Designation of transitions as in Figure 4. All energies in cm^{-1}

$[(en)_2Cr(OH)_2Cr(en)_2]Cl_4\cdot 2H_2O$

Absorption	Δ	Luminescence	Δ
A_0 14 080		A_0 14 078	
		A_1 14 046	32
A_2 13 984	96	A_2 13 983	63
		A_3 13 886(?)	97
B_0 14 247			
B_1 14 214	33		

$[(en)_2Cr(OH)_2Cr(en)_2]Br_4\cdot 2H_2O$

Absorption	Δ	Luminescence	Δ
A_0 14 059		A_0 14 059	
A_1 14 027	32	A_1 14 030	29
A_2 13 967	60	A_2 13 967	63
		A_3 13 876(?)	91
B_0 14 232			
B_1 14 201	31		
B_2 14 140	61		

$[(en)_2Cr(OH)_2Cr(en)_2]I_4$

Absorption	Δ	Luminescence
A_0 14 167		
A_1 14 143	24	
A_2 14 096	47	A_2 14 096
B_0 14 325		
B_1 14 300	25	
C_0 14 330		
C_1 14 304	26	
C_2 14 252(?)	52	

$[(en)_2Cr(OH)_2Cr(en)_2]Cl_2[ClO_4]_2\cdot 2H_2O$

Absorption	Δ	Luminescence	Δ
A_0 14 125		A_0 14 127	
A_1 14 096	29	A_1 14 096	31
A_2 14 044	52	A_2 14 043	53
		A_3 13 979(?)	64
B_0 14 308			
B_1 14 279	29		
B_2 14 225	54		
B_3 14 167	58		
C_0 14 336			
C_2 14 256	80		
C_3 14 192	64		

bility data of the iodide salt with a susceptibility curve calculated from the spectroscopically determined exchange parameters. This behaviour is typical of the complexes investigated. Since all the spectroscopic values were determined at <40 K, this discrepancy can be taken as an indication that *J* is slightly temperature dependent, increasing by a few percent on cooling from room to helium temperature. A similar behaviour has been found in $[(H_3N)_5Cr(OH)Cr(NH_3)_5]Cl_5\cdot H_2O$ by the use of neutron inelastic scattering.[11]

Table 11 confirms the statement made before that the values of the biquadratic exchange parameter *j* obtained from the least-squares fit of the magnetic data have little physical significance. It is clear that a temperature dependence of *J*, and changes of 5—10% in *J* between room and helium temperature that have been found to occur,[11,12] will be taken up by the adjustable parameters *j* and *g* in the fitting process. While the spectroscopic *j* values of the chloride, bromide, and iodide salts are within $\leqslant 1\%$ of *J*, the chloride perchlorate salt has an exceptionally large positive *j*.

Similarly large *j* values have been found for a number of Cr^{3+} and Mn^{2+} pairs in diamagnetic host lattices.[9,10] The *j* values expected from Anderson's theory of superexchange are within $\leqslant 1\%$ of *j*.[18] Exchange striction rather than biquadratic exchange has therefore been discussed as a possible source of the large *j* parameters.[10,19] Magnetostriction is well known in condensed magnetic materials. It is unfortunate that the exact low-temperature geometry of the $[(en)_2Cr(OH)_2Cr(en)_2]^{4+}$ complex in the chloride perchlorate salt is not known. A comparison with the geometries of the other salts and a possible analysis of the large *j* value are therefore not possible. But it is quite clear that exchange striction is a much more likely cause than biquadratic exchange because the latter is not expected to show such a large variation for the same binuclear complex.

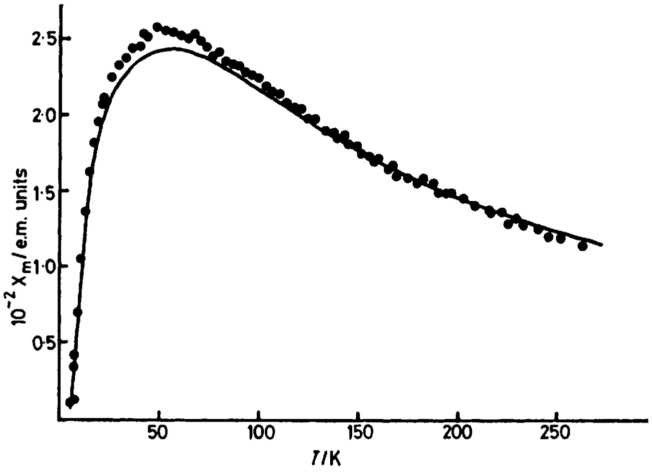

FIGURE 9 Magnetic-susceptibility data for $[(en)_2Cr(OH)_2Cr(en)_2]I_4$ (●). The full line corresponds to a calculation using the spectroscopically determined exchange parameters, $J = 24.3$ cm^{-1}, $j = 0.083$ cm^{-1}, and $g = 2.0$. The discrepancy indicates a temperature dependence of *J*. It would be more pronounced if a slightly smaller and thus more realistic *g* value had been used for the calculation

Besides the magnetic data, Table 11 contains some structural data for $[(en)_2Cr(OH)_2Cr(en)_2]^{4+}$ in four complexes of known crystal structure. An empirical correlation between structural and magnetic parameters is not straightforward, because Cr–O distances have to be considered as well as Cr–O–Cr angles. The present data do not fit the correlation of *J* values and Cr–O–Cr angles for di-μ-hydroxo-bridged chromium complexes, $[L_4Cr(OH)_2CrL_4]$, made by Hodgson and his co-workers.[1] The exchange interactions have a subtle dependence on the nature of the ligands L, which is not fully reflected by the Cr–O–Cr angle. Since a very broad range of *J* values can be obtained within a series of complexes containing $[(en)_2Cr(OH)_2Cr(en)_2]^{4+}$, it is desirable to collect more data within this series, thus eliminating the problems of varying the ligands L.

TABLE 11

Exchange parameters for various salts of $[(en)_2Cr(OH)_2Cr(en)_2]^{4+}$. The magnetic values were obtained by fitting the magnetic-susceptibility data with a Hamiltonian $\hat{H}_{ex} = J(\hat{S}_a . \hat{S}_b) - j(\hat{S}_a . \hat{S}_b)^2$. The three parameters J, j, and g were refined. Spectroscopic values were obtained from the experimental splittings of Table 10. The eigenvalues of the above Hamiltonian are given by $E(S) = \frac{J}{2}\left[S(S+1) - \frac{15}{2}\right] - \frac{j}{4}\left[S^2(S+1)^2 - 15S(S+1) + \frac{225}{4}\right]$

Anions of $[(en)_2Cr(OH)_2Cr(en)_2]^{4+}$ salt	Magnetic			Spectroscopic		Structural				
	J/cm^{-1}	j/cm^{-1}	g	J/cm^{-1}	j/cm^{-1}	Cr–OH–Cr/°	Cr–O/Å	Cr–Cr/Å	OH–O/Å	R Factor
$[S_2O_6]_2$ (ref. 5)	2.16 ±0.04	0.234 ±0.007	1.947 ±0.007			100.0 ±0.2	1.980 ±0.005 1.978 ±0.005	3.032 ±0.003	2.724 ±0.009	0.049
$Cl_4 \cdot 2H_2O$	29.4 ±0.5	0.3 ±0.1	1.978 ±0.005	31.4 ±0.4	0.08 ±0.02	102.42 ±0.05	1.941 ±0.001 1.949 ±0.001	3.030 ±0.001	2.610 ±0.002	0.023
$Br_4 \cdot 2H_2O$	27.7 ±0.8	0.3 ±0.2	1.976 ±0.008	30.0 ±0.3	0.11 ±0.08	102.64 ±0.11	1.946 ±0.002 1.946 ±0.002	3.038 ±0.005	2.627 ±0.005	0.031
$Cl_2[ClO_4]_2 \cdot 2H_2O$	24.8 ±0.3	0.4 ±0.1	1.963 ±0.004	22.2 ±0.2	1.12 ±0.06	103.42 ±0.08	1.946 ±0.002 1.952 ±0.002	3.059 ±0.002	2.658 ±0.003	0.044
I_4	21.5 ±0.4	0.4 ±0.1	1.967 ±0.004	24.3 ±0.9	0.1 ±0.2					

Our results are at variance with the magnetochemical properties of the chloride, bromide, and iodide salts of $[(en)_2Cr(OH)_2Cr(en)_2]^{4+}$ reported by Jasiewicz *et al.*[4] Since the powders used in that study were not characterized by elemental analysis we cannot explain the large discrepancies.

EXPERIMENTAL

Preparations.—The complexes $[Cr_2(OH)_2(en)_4]Cl_4 \cdot 2H_2O$ (Found: C, 17.4; H, 6.70; Cl, 25.65. Calc.: C, 17.25; H, 6.90; Cl, 25.5; N, 20.15%) and $[Cr_2(OH)_2(en)_4]Br_4 \cdot 2H_2O$ (Found: C, 13.1; H, 5.30; Br, 43.75; N, 15.35. Calc.: C, 13.1; H, 5.20; Br, 43.55; N, 15.25%) were prepared according to the literature methods.[20]

$[Cr_2(OH)_2(en)_4]I_4$. The pure bromide salt (3 g) was suspended in an aqueous solution (7 cm^3) of $[NH_4]I$ (150 g of $[NH_4]I$ in 100 cm^3 of water) and stirred for 90 min. The product was filtered off and purified by dissolution in 0.01 mol dm^{-3} HI solution (800 cm^3), filtration through a micropore filter, and addition of $[NH_4]I$ solution (6 cm^3). Slow cooling to 2 °C yielded 2.2 g of the iodide. After twice repeating the purification procedure the product was dried over H_2SO_4. An analytically pure product was thus obtained (Found: C, 10.45; H, 4.05; I, 55.35. Calc.: C, 10.4; H, 4.15; I, 55.5; N, 12.15%).

$[Cr_2(OH)_2(en)_4]Cl_2[ClO_4]_2 \cdot 2H_2O$. A 1.1 mol dm^{-3} aqueous solution of $[NH_4][ClO_4]$ was allowed to slowly diffuse into a saturated solution of the chloride salt (Found for product: C, 14.25; H, 5.55; Cl, 20.7; N, 16.4. Calc.: C, 14.05; H, 5.60; Cl, 20.75; N, 16.4%).

The crystals of $[Cr_2(OH)_2(en)_4]Cl_4 \cdot 2H_2O$ and $[Cr_2(OH)_2(en)_4]Br_4 \cdot 2H_2O$ used for the crystallographic work were grown at 4 °C by letting a 3.5 mol dm^{-3} solution of $[NH_4]Cl$ or $[NH_4]Br$ diffuse slowly into a saturated aqueous solution of the respective complexes. Mixed bromide chloride crystals may also be obtained. Crystals large enough for single-crystal optical spectroscopy could be grown for the chloride, bromide, and chloride perchlorate salts by slow diffusion of a concentrated solution of the respective anion into a solution containing the binuclear complex.

X-*Ray Measurements, Data Reduction, and Structure Determination.*—Single-crystal X-ray intensity measurements were collected on a Syntex $P2_1$ automatic diffractometer equipped with a molybdenum tube ($\lambda = 0.710\ 69$ Å). Unwanted radiation was eliminated by a niobium filter. A scan was made up to 1° on each side of the calculated $K\alpha_1/K\alpha_2$ doublet; at each end of this interval the stationary background was measured for 25% of the scan time. The scan rate varied between 2 and 10° min^{-1}, depending on the intensity of the reflection. Analysis of the profiles was performed by the modified Lehmann–Larsen algorithm.[21]

The 'X-ray '72' system of programs [22] was used for the data reduction and the determination of the structures. Drawings were plotted by means of the ORTEP program.[23] Neutral scattering factors [24] for Cr, O, N, C, and H were used, whilst for Br and Cl anionic ones were preferred. Anomalous dispersion corrections [25] were applied for Br, Cr, and Cl.

Magnetic-susceptibility Measurements.—All the measurements were made on polycrystalline samples using a moving-sample technique.[26] Details of the apparatus are given in ref. 27. The temperature was measured by means of a chromel/gold–iron thermocouple, calibrated as described in the literature.[28] The estimated accuracy of the temperature measurements is ±0.2 K. Nickel was used for the calibration of the susceptibility. The estimated error of the susceptibility measurements is ±0.7%. No field dependence was detected. The magnetic field, which, for all the measurements, was in the order of 1 T, had an estimated stability of ±0.001 T.

Spectroscopic Measurements.—Absorption spectra were recorded for single crystals and Nujol mulls using a Cary 17 spectrometer equipped with a red-sensitive photomultiplier tube. Luminescence spectra were obtained for freshly prepared and recrystallized polycrystalline samples. A 150-W sealed-beam xenon lamp and a Spex Minimate monochromator were used for the excitation. A 0.75 m Spex single monochromator equipped with a grating blazed at 750 nm was used for the dispersion of the luminescence. A RCA 31034 photomultiplier tube, cooled to -30 °C, was used for detection. Cooling of the sample was achieved by a helium-gas flow technique. Any temperature in the range 6—300 K could thus be easily obtained. The temperature was measured with a chromel/gold–iron thermocouple, the estimated accuracy being ± 1 K.

We thank the Swiss National Science Foundation for support, K. Mattenberger and O. Vogt, Laboratorium für Festkörperphysik, ETH, Zürich, for the magnetic-susceptibility measurements, and H. Wagner, Ciba-Geigy Analytical Laboratories, Basel for elemental analyses.

[8/1024 *Received*, 1*st June*, 1978]

REFERENCES

[1] R. P. Scaringe, W. E. Hatfield, and D. J. Hodgson, *Inorg. Chem.*, 1977, **16**, 1600 and refs. 17—21 therein.

[2] P. J. Hay, J. C. Thibeault, and R. Hoffmann, *J. Amer. Chem. Soc.*, 1975, **97**, 4884.

[3] D. J. Hodgson, *Progr. Inorg. Chem.*, 1975, **19**, 173.

[4] B. Jasiewicz, M. F. Rudolf, and B. Jezowska-Trzebiatowska, *Acta Phys. Pol.*, 1973, **A44**, 623.

[5] S. J. Cline, R. P. Scaringe, W. E. Hatfield, and D. E. Hodgson, *J.C.S. Dalton*, 1977, 1662.

[6] B. Bleaney and K. D. Bowers, *Proc. Roy. Soc.*, 1952, **A214**, 451.

[7] J. Ferguson, H. U. Güdel, and M. Puza, *Austral. J. Chem.*, 1973, **26**, 505, 513.

[8] J. Ferguson and H. U. Güdel, *Chem. Phys. Letters*, 1972, **17**, 547.

[9] H. van den Boom, A. J. J. van Dijsseldonk, and J. C. M. Henning, *J. Chem. Phys.*, 1977, **66**, 2369 and refs. 6 and 11 therein.

[10] J. Owen and E. A. Harris, in 'Electron Paramagnetic Resonance,' ed. S. Geschwind, Plenum, New York, 1972, p. 427.

[11] H. U. Güdel and A. Furrer, *Mol. Phys.*, 1977, **33**, 1335.

[12] A. Furrer and H. U. Güdel, *Helv. Phys. Acta*, 1977, **50**, 439.

[13] Karen Kaas, *Acta Cryst.*, 1976, **B32**, 2021.

[14] W. C. Hamilton and J. A. Ibers, 'Hydrogen Bonding in Solids,' W. A. Benjamin, New York, 1968, p. 16.

[15] L. Pauling, 'The Nature of the Chemical Bond,' Cornell University Press, Ithaca, New York, 1960, p. 260.

[16] S. C. Abrahams and E. T. Keve, *Acta Cryst.*, 1971, **A27**, 157.

[17] 'International Tables of *X*-Ray Crystallography,' Kynoch Press, Birmingham, 1974, vol. 4, pp. 293—295.

[18] P. W. Anderson, in 'Solid State Physics,' eds. F. Seitz and D. Turnbull, Academic Press, New York, 1963, vol. 14, p. 99.

[19] K. N. Shrivastava, *Phys. Letters*, 1976, **A56**, 399.

[20] J. Springborg and C. E. Schaffer, *Inorg. Synth.*, 1978, **18**, 75.

[21] D. Schwarzenbach, *Abs. 4th European Cryst. Meeting*, Oxford, 1977, PI.20.

[22] The '*X*-Ray' System, Version of D. Schwarzenbach, Technical Report TR-192, Computer Science Center, University of Maryland, College Park, Maryland, 1972.

[23] C. K. Johnson, ORTEP, Oak Ridge National Laboratory, Oak Ridge, Tennessee, 1971.

[24] D. T. Cromer and J. Mann, *Acta Cryst.*, 1968, **A24**, 321; R. F. Stewart, E. R. Davidson, and W. T. Simpson, *J. Phys. Chem.*, 1965, **42**, 3175.

[25] D. T. Cromer and D. L. Libermann, *J. Chem. Phys.*, 1970, **53**, 1891.

[26] O. Vogt, unpublished work.

[27] J. P. Rebouillat, Thèse de docteur, C.N.R.S., Grenoble, 1972.

[28] R. Rosenbaum, *Rev. Sci. Instr.*, 1968, **39**, 890.